



ELSEVIER

Available online at www.sciencedirect.com

SCIENCE @ DIRECT®

 AGRICULTURAL
 AND
 FOREST
 METEOROLOGY

Agricultural and Forest Meteorology xxx (2005) xxx–xxx

www.elsevier.com/locate/agrformet

Determining digital hemispherical photograph exposure for leaf area index estimation

 Yongqin Zhang^{a,*}, Jing M. Chen^a, John R. Miller^b
^a University of Toronto, 100 St. George St., Room 5047, Toronto, Ont., Canada M5S 3G3

^b York University, 4700 Keele Street, Toronto, Ont., Canada M3J 1P3

Received 18 January 2005; accepted 15 September 2005

Abstract

A correct exposure is of crucial importance for accurate retrieval of canopy parameters using hemispherical photograph techniques. Digital hemispherical photographs were collected under different sky brightness conditions using a Nikon CoolPix 4500 camera with an FC-E8 fish-eye lens for canopies of different species and openness. Different exposure schemes were employed to investigate the effects of photographic exposure on the estimations of the effective leaf area index (L_e) and gap fraction. The contrast between the sky and foliage under each exposure scheme was calculated to determine the correct exposure under different weather conditions. The results demonstrated that digital hemispherical photographs taken with automatic exposure are not reliable, causing L_e underestimations by 16–71% for medium and high density canopies ($L_e = 3.2$ –4.8) and corresponding gap fraction overestimations by 18–72%. While for open canopies with $L_e < 1.26$, L_e was overestimated by 11–29%, and the corresponding gap fraction was underestimated by 4–28%. Studies showed that increasing one stop of exposure results in 3–28% differences in L_e for canopies with different openness. Based on the analysis, we determined the optimum exposure and developed a protocol for acquiring digital hemispherical photos. The protocol requires first measuring reference exposure for the open sky using a built-in camera light meter, and then take photographs inside the canopy using the same camera with two stops of more exposure than the reference exposure in order to make the sky appear white and consequently also maximize the contrast between the sky and foliage. This protocol is applicable for different sky brightness and for different canopy openness. In dense canopies, this procedure requires much less exposure than automatic exposure, but in very open canopies, this procedure requires more exposure than the automatic exposure. Using the exposure determined with this procedure rather than the automatic exposure, the comparison of L_e values from the LAI-2000 and digital photographs is greatly improved, with R^2 increasing from 0.77 to 0.95, and RMSE decreasing from 1.29 to 0.38.

© 2005 Published by Elsevier B.V.

Keywords: Digital hemispherical photographs; Exposure; Leaf area index; Gap fraction

1. Introduction

Leaf area index (LAI) is defined as half the total green leaf area per unit ground surface area (Chen and Black,

1992). It is a critical canopy structural parameter required in ecological and process-based canopy photosynthesis models (Amiro et al., 2000; Chen et al., 1999; Kimball et al., 1997; Liu et al., 1997, 2002; Running and Hunt, 1993). The LAI of a canopy determines light, thermal and moisture conditions within the canopy, and thus influences its carbon, water, and energy balances (Fassnacht et al., 1994). Direct and indirect methods are often used for determining LAI (Fassnacht et al., 1994; Gower et al., 1999; Jonckheere et al., 2004;

* Corresponding author. Tel.: +1 416 978 7085; fax: +1 416 946 7715.

E-mail addresses: zhangy@geog.utoronto.ca (Y. Zhang), chenj@geog.utoronto.ca (J.M. Chen).

Mussche et al., 2001; Rich et al., 1993; Weiss et al., 2004). Indirect methods, which use optical instruments such as tracing radiation and architecture of canopies (TRAC), LAI-2000 (Plant Canopy Analyzer, LI-COR, Lincoln, NE), are widely adopted for LAI acquisition due to their fast and non-destructive nature. A combination of these two instruments is suggested for accurate LAI measurements (Chen et al., 1997).

Hemispherical or fish-eye photography is another common means for measuring LAI as well as studying the canopy architecture and solar radiation in forests (Easter and Spies, 1994; Englund et al., 2000; Frazer et al., 2001; Wagner, 2001). Hemispherical photographs capture the light obstruction/penetration patterns in the canopy, from which the canopy architecture and foliage area can be quantified (Chen et al., 1991; Fournier et al., 1996; Nilson, 1999; Ross, 1981). Hemispherical photographs have the advantage of spatial discrimination, and are particularly useful for acquiring foliage angular distributions, and gap fractions at different zenith and azimuthal angles. Gap fraction is generally calculated from the photographs to quantify canopy openness and architectures. The plant area index (including both green and non-green canopy materials) and the leaf inclination angle distribution of a canopy can be simultaneously calculated by measuring gap fractions at several zenith angles (Chen et al., 1991). By dividing each annulus into small segments, the 3D canopy structure and its angular variations can be quantified (van Gardingen et al., 1999).

A good correlation has been found between film and digital systems in open canopies under overcast sky conditions for estimating canopy structure, light transmission, and LAI (Englund et al., 2000; Frazer et al., 2001). With the development of affordable digital technologies, digital cameras have been widely used to replace conventional film cameras for hemispherical photograph acquisition. Digital hemispherical photographs are less expensive and can be acquired with greater ease and convenience. Digital photographs can be kept as permanent records of the measurements while eliminating errors in film development and image scanning (Chen et al., 1991; Mussche et al., 2001). It has been found that conventional film hemispherical photography produces inaccurate estimations of canopy openness and light transmission when the stands are dense with many small gaps (canopy openness is less than 10%) (Frazer et al., 2001; Machado and Reich, 1999; Roxburgh and Kelly, 1995). High-resolution digital photographs can distinguish leaf area from sky area more accurately than photographic films and avoid the aggregation of pixels in images with lower

resolutions (Blennow, 1995). The availability of computer software for image processing allows efficient use of digital hemispherical photos. Digital photos can also be used to derive vegetation clumping index, which characterizes the spatial distribution of foliage, and thus the actual LAI, by adopting the gap size distribution theory used in the TRAC instrument (Leblanc et al., 2005). Both the LAI-2000 and hemispherical photographs make use of diffuse light. Compared with the LAI-2000, hemispherical photographs can provide detailed information about the canopies. A digital hemispherical camera can potentially substitute for the LAI-2000 instrument to provide accurate LAI measurements, if operated appropriately.

Although hemispherical photography is believed to be an efficient way for long-term arid ecosystem monitoring and LAI measurements, the accuracy and reliability of digital hemispherical photographs for LAI and canopy structure estimations need to be assessed systematically. Compared with destructive harvest results, LAI obtained from digital hemispherical photographs was found to be underestimated by 50% (Brenner et al., 1995; Sommer and Lang, 1994). Even with the segmented method, which divides each annulus into a number of small segments, the underestimation cannot be completely eliminated (van Gardingen et al., 1999).

Camera exposure settings influence the estimation of light transmission and LAI and are demonstrated as a major cause of measurement errors (Chen et al., 1991; Englund et al., 2000; Macfarlane et al., 2000; Wagner, 1998). Photography exposure influences the grey value of unobscured pixels, which are used as a reference for discriminating completely and partly obscured pixels (Wagner, 1998, 2001). It can also result in a discrepancy in the canopy openness derived from digital and film techniques (Englund et al., 2000). It is found that the estimated effective leaf area index (L_e) from film-based camera decreases with the increase of photographic exposure (Chen et al., 1991; Macfarlane et al., 2000). Olsson et al. (1982) suggested the use of a spot light meter, instead of the film camera's built-in exposure meter, for obtaining the right exposure regardless of canopy openness. Chen et al. (1991) proposed the use of the unobstructed zenith area of overcast sky as a standard reference and 1–2 stops more exposure relative to the brightness of the sky for measuring LAI inside the canopy. An overexposure of three stops relative to the sky reference was advised as the best exposure setting for measuring the light transmission through achieving the sky uniformity (Clearwater et al., 1999; Wagner, 1998). So far, a standard exposure setting for digital

151 hemispherical photography has not been verified for
 152 LAI measurements, and no systematic study has been
 153 reported for this purpose. It is found that for film-based
 154 hemispherical photos, even one stop exposure can
 155 influence the LAI estimation by 13% (Macfarlane et al.,
 156 2000). Compared with the logarithmic response of film
 157 cameras to light, digital cameras have the advantage of a
 158 linear response, which effectively lighten the midtone
 159 pixels (Covington Innovations, 2004). Digital hemi-
 160 spherical systems are found to be more sensitive to sky
 161 conditions and produce much higher estimations for
 162 canopy openness and lower effective LAI estimations
 163 than film systems (Englund et al., 2000; Frazer et al.,
 164 2001). It is suggested that the digital system may be
 165 more sensitive than film system to exposure, particu-
 166 larly at low light levels (Hale and Edwards, 2002). To
 167 accurately estimate forest LAI and canopy structural
 168 parameters using digital cameras, researchers called for
 169 a standardized protocol for exposure setting for
 170 acquiring hemispherical photographs (Jonckheere
 171 et al., 2004).

173 The objectives of this paper are (1) to summarize the
 174 theoretical basis of photograph exposure for optimum
 175 measurements of canopy architectural parameters; (2)
 176 to investigate whether the maximum contrast between
 177 sky and foliage in the photograph would be the criterion
 178 for setting the optimum exposure using field data from
 179 forest stands of various types and densities; and (3) to
 180 propose a protocol for determining digital photograph
 181 exposure for LAI and gap fraction estimations based on
 182 this investigation.

183 2. Exposure theory of digital cameras

184 The photochemical reaction taking place during
 185 exposure obeys the reciprocity law (Bunsen and
 Roscoe, 1862), i.e. the exposure E may be expressed as:

$$188 E = I \times T \quad (1)$$

189 where I is the illuminance in lux (metric quantity),
 190 which is the intensity of the light acting upon the
 191 sensitized photographic material, and T is the time that
 192 this illumination acts on the photographic material. The
 193 reciprocal law states that the illumination time and the
 194 irradiance level are reciprocal for induction of a photo-
 195 chemical effect, i.e. an exposure at a high irradiance for
 196 a short time is photochemically equivalent to an expo-
 197 sure at a low intensity for a long time. Exposure in a
 198 camera is determined by two settings: the shutter speed
 199 and the lens aperture. The length of time that the
 200 photosensitive material is exposed (shutter speed) is
 inversely proportional to the amount of light hitting the

surface (lens aperture). When taking photographs, the
 shutter speed and aperture can be traded to yield the
 same exposure. Decreasing the shutter speed by one
 stop has the same effect on exposure as increasing the
 lens aperture by one stop.

206 This reciprocity is a reliable rule for most typical
 207 shutter speeds. However, at very slow or, more
 208 conversely, very fast shutter speeds, photosensitive
 209 materials do not respond linearly as predicted and the
 210 law of reciprocity does not hold. Digital cameras are
 211 designed to mimic film response to light, but the
 212 response pattern can be significantly different from
 213 films. Digital cameras acquire photographs using a
 214 couple charge device (CCD) matrix, which is a light-
 215 sensitive integrated circuit placed at the focal plane of
 216 an optical imaging system. Digital cameras respond to
 217 light linearly from a lower threshold to an upper
 218 threshold exposure. After the upper threshold, the
 219 digital response is saturated (Fig. 1). In comparison,
 220 film's response to exposure shows gradual variations at
 221 both low and high exposures (Norman, 2003). The
 222 linear response range of digital cameras shown in Fig. 1
 223 is larger than that of films, but this may be camera
 224 dependent. The difference in the light response pattern
 225 between films and digital media suggests that we need
 226 to re-evaluate exposure theories developed for films for
 227 use in digital cameras.

228 It has been discovered that the average scene reflects
 229 18% of the light that falls on it (Unwin, 1980). All the
 230 light meters, film and now digital cameras are designed
 231 to have an automatic mode. The camera's built-in light
 232 meter reads the reflected light from objects and adjusts
 233 the combination of shutter speed and aperture to get an

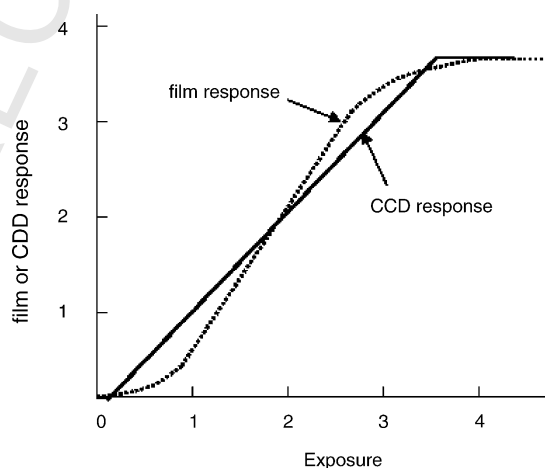


Fig. 1. Schematic diagram for characteristic curves of the response of digital and film media to exposure (both axes are on logarithmic scales).

233 18% gray tone on the photograph. The automatic
 234 exposure mode guarantees exposure settings that
 235 reproduce objects at a medium gray level of 18%
 236 brightness. But when taking digital hemispherical
 237 photographs inside a canopy, the large contrast between
 238 the bright sky and dark canopy components creates a
 239 significant potential of incorrect exposure using
 240 automatic settings. The spatial heterogeneity of the
 241 scene can cause underexposure or overexposure. Under-
 242 exposure can result in a loss of details in the dark
 243 subjects, while overexposure can result in a loss of
 244 detail in bright objects. As the automatic exposure
 245 varies with the average sky brightness and canopy
 246 openness, a significant error in the determination of LAI
 247 may be introduced when the sky luminance is not
 248 uniform with respect to the zenith angle.
 249

250 The illuminance measured with a photometer can be
 251 converted to camera exposure based on the formula
 252 proposed by Unwin (1980), which assumes the scene as
 253 an 18% gray body. Based on this formula, Chen et al.
 254 (1991) suggested that the optimum exposure inside a
 255 vegetation canopy would be 1–2 stops larger than the
 256 reference exposure found outside the stand in order to
 257 make sky appear white. Theoretically, 2.5 stops of
 258 overexposure are required to make an unobscured
 259 overcast sky appear completely white, i.e. increasing
 260 the reflectivity from 18 to 100% (one stop to increase to
 261 36%, two stops to increase to 72%, and three stops to
 262 increase to 144%) (Macfarlane et al., 2000). Chen et al.
 263 (1991) postulated that 1–2 stops rather than 2–3 stops of
 264 overexposure compared with sky reference are needed
 265 possibly because of multiple scattering in the canopy
 266 which enhances the brightness of foliage in the
 267 photograph. However, this suggested exposure setting
 268 has not been systematically tested for either film or
 269 digital cameras. For digital cameras, one criterion for
 270 the optimum exposure inside the canopy is to make use
 271 of the full digital range to capture the scene
 272 components, i.e. the foliage appears black (digital
 273 number (DN) = 0) and the sky background appears
 274 white (DN = 255). In practice, the optimum exposure
 275 for hemispherical photographs in a forest canopy should
 276 make the sky appear as white as possible and in the
 277 meantime the canopy components as dark as possible.
 278 Thus for the optimum exposure, the relative contrast
 279 between the sky pixels and foliage pixels should
 280 theoretically approach the maximum.

281 Photographs require more exposure in dense than in
 282 open stands, therefore analysis on the influences of the
 283 digital camera exposure on LAI and gap fraction
 284 estimations is necessary for determining an optimal
 285 exposure for different stand structures and sky cond-

itions. A reliable way to determine the optimum 286
 exposure is to measure hemispherical sky brightness 287
 and then adjust the camera settings accordingly. This 288
 sky reference reading should be made in a large opening 289
 outside the forest stand, which provides an unobstructed 290
 sky view up to the 75° zenith angle in all azimuthal 291
 directions. With experience in angular variations of sky 292
 radiance, this reference reading can also be made in 293
 small openings (Clearwater et al., 1999; Wagner, 1998, 294
 2001). When the camera's aperture size is fixed to 295
 ensure a consistent field of view, a decrease of the 296
 camera's shutter speed by 2–3 stops will provide the 297
 desired exposure. The following experiments were 298
 conducted to explore the effects of exposure and test 299
 whether this simple rule of decreasing the shutter speed 300
 by two or three stops relative to a sky reference reading 301
 can be the most appropriate exposure for leaf area index 302
 estimation. In this operation, it is critical that the same 303
 camera is used for both sky reference reading and 304
 photograph acquisition inside a stand as the camera 305
 automatic exposure reading may differ by a few to 306
 several stops (Chen et al., 1991). 307

3. Experiments and methods 308

3.1. Study site description 309

Experiments were conducted in one deciduous and 310
 three coniferous stands of different canopy openness. 311

One sugar maple stand (*Acer Saccharum*) was 312
 selected in Haliburton Forest, Ontario (45°14'15.5"N, 313
 78°32'18.0"W). The average diameter at breast height 314
 (DBH) for the dominant, co-dominant and suppressed 315
 trees were, respectively, 51.9, 35.0, and 20.4 cm. Three 316
 50 m-long transects separated by 10 m were set up in 317
 the east–west direction. Each transect was marked every 318
 10 m using forestry flags for location identification. 319

One mature Douglas-Fir stand was near the Camp- 320
 bell River on Vancouver Island, which is one of tower 321
 flux stations of Fluxnet Canada Research Network 322
 (49°54'18.0"N, 125°21'57.6"W). A 400 m transect was 323
 set up in the SW-NE direction. The transect was divided 324
 into two portions using the flux tower as the midway 325
 marker and forestry flags were also used every 10 m 326
 along the transect. 327

Two black spruce (*Picea Mariana*, abbreviation SB) 328
 stands in Sudbury: SB1 at 47°09'45.3"N, 81°44'44.3"W 329
 and SB2 at 47°12'9.4" to 81°54'30.3"W, were investi- 330
 gated. These two stands have different canopy closure 331
 and growth conditions. The SB1 stand is relatively young 332
 and has a vigorous understory including Labrador tea, 333
 blueberry, and bog rosemary. The dominant understory in 334

334
 335 SB2 includes moss and Labrador tea under a mature
 336 canopy. Ten trees at each site were selected to measure
 337 the tree height and DBH. The average tree heights of the
 338 SB1 and SB2 were 4.53 ± 1.507 and 14.04 ± 2.012 m,
 339 and the DBH were 4.98 ± 2.157 and 16.71 ± 3.358 cm,
 340 respectively. For each stand, two 50 m parallel transects
 341 separated by 20 m were set up in the east-west direction,
 342 marked every 10 m by forestry flags.

3.2. Experimental methods

343
 344 On top of forestry flags in the four stands, a series of
 345 photographs using different exposure settings were
 346 taken to evaluate the effect of exposure and sky
 347 brightness on the accuracy of forest structure estimation.
 348 All hemispherical photographs were taken with the
 349 high-resolution (4 Mega pixels) Nikon CoolPix 4500
 350 digital camera, which has a large range of shutter speed.
 351 Compared with previous models such as CoolPix 950,
 352 the Nikon CoolPix 4500 has less chromatic aberration
 353 (e.g. *Digital Photography Review*, 2003; Frazer et al.,
 354 2001). A Nikon FC-E8 fish-eye lens with a field of view
 355 of 183° was attached to the camera. The camera was
 356 mounted on a tripod to facilitate a horizontal camera
 357 setting.

358 As the interference of direct sunlight can cause errors
 359 of up to 50% (Welles and Norman, 1991), all the
 360 photographs were taken under uniform sky conditions
 361 (overcast weather) or near sunset or sunrise. The
 362 following cameras settings were chosen before the
 363 measurements (for Nikon CoolPix 4500, and may vary
 364 for other cameras): (1) manual mode; (2) Fish-eye 1 lens
 365 (fixed with centrally weighted exposure for automatic
 366 exposure); (3) in the manual mode, aperture fixed at
 367 F5.3; (4) high image quality (2272×1704 pixels), and
 368 (5) JPEG format (no difference in digital values was
 369 found between JPEG and TIFF format, Frazer et al.,
 370 2001).

371 Our experiments were conducted under different sky
 372 brightness conditions to analyze variations of the image
 373 contrast with exposure. Photographs were taken starting
 374 from the sky reference exposure up to the automatic
 375 exposure. For example, if the sky reference exposure
 376 time were determined to be 1/1000 s (F5.3), a series of
 377 photographs would be taken with the aperture fixed at
 378 F5.3 and the shutter speed decreasing systematically
 379 from 1/1000, 1/500, 1/250, and 1/125 to 1/60 s, until the
 380 shutter speed indicator corresponded to the automatic
 381 exposure. Hemispherical photographs were taken near
 382 sunset on 27 May 2004 for the sugar maple stands along
 383 one transect. The sky exposure before and after the
 384 measurements was respectively 1/500 s (F5.3) at 18:40

384
 385 p.m. and 1/250 s (F5.3) at 19:55 p.m. On 25 August
 386 2004, along the 400 m transect in the Douglas-Fir stand,
 387 series of photographs were collected under overcast
 388 conditions at every 50 m markers. The sky exposure
 389 before and after the measurements was 1/2000 s (F5.3)
 390 at 15:20 p.m. and 1/1000 s (F5.3) at 16:45 p.m. local
 391 time. Hemispherical photographs were collected on
 392 overcast days from 7th to 12th August 2004 at the SB1
 393 and SB2 stand. The sky conditions were ideally stable at
 394 1/1000 s (F5.3) before and after the measurements for
 395 both stands.

396 The LAI-2000 instrument was used to measure L_e at
 397 approximately the same time as hemispherical photo-
 398 graphs. A 90° view restrictor was used to block the
 399 influence of the operator and bright sky near sunset
 400 behind the operator. LAI-2000 measurements were
 401 taken at nearly the same position and the same height of
 402 the fish-eye lens so that L_e results from two measure-
 403 ments can be compared.

3.3. Digital image processing

404
 405 Hemispherical photographs in the JPEG format have
 406 three 8-bit image channels (red, green, and blue),
 407 producing a DN range from 0 to 255. In the blue band of
 408 the electromagnetic spectrum, foliage elements have the
 409 lowest reflectivity and transmittance, making the
 410 foliage in the blue band darker than in the red or green
 411 band. To minimize the interference of multiple
 412 scattering in the canopy and chromatic aberration, only
 413 the blue band of photographs was used in our analysis.
 414 For the Nikon CoolPix 4500, the diameter of the 180°
 415 circular projected hemispherical photographs was
 416 estimated to be 1590 pixels. To calculate the within
 417 pixel gap fraction, the digital hemispherical photo-
 418 graphy (DHP) software was used to process images
 419 (Leblanc, 2003; Leblanc et al., 2005) instead of the
 420 time-saving automatic thresholding method (Nobis and
 421 Hunziker, 2005). In the DHP software, techniques for
 422 film-based hemispherical photographs proposed by
 423 Wagner (1998, 2001) were adopted and applied for
 424 digital photographs. The software analyzes fixed
 425 zenithal annulus segments and divides the images into
 426 up to ten rings. Two thresholds are used for each annulus
 427 to distinguish leaf from sky. By setting two threshold
 428 gray values, a blue channel image is classified as
 429 completely transparent, completely obscured, and parti-
 430 ally obscured pixels, to represent sky, foliage, and
 431 mixed sky and foliage pixels, respectively. The thresh-
 432 olds are set where the histogram digital number values
 433 start to deviate from the straight line in the logarithmic
 434 plot (Fig. 2). When no linear part can be found on the

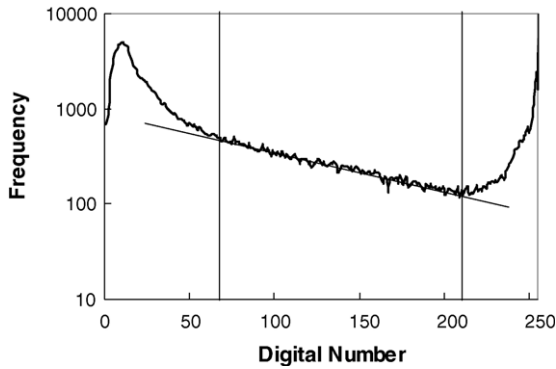


Fig. 2. Digital number histogram of a nine-degree annulus from a single digital hemispherical photograph. The y-axis is in a logarithm scale to demonstrate the mixed pixel part of the histogram found between the two thresholds ($DN_{\min} = 71$, $DN_{\max} = 212$). DN_{\min} and DN_{\max} are respectively determined where the linear part of the histogram in a logarithm starts and ends.

434

435 histogram, the visual inspection of the image under the
436 colour mode can be compared to the original 8-bit blue
437 channel to find the correct thresholds. For mixed pixels
438 between the two thresholds, the program uses the
439 linearity of the camera CCD array to calculate the
440 within pixel gap fraction using a linear unmixing
441 procedure (Leblanc et al., 2005).

442 Image misclassification is known to be a source of
443 error for LAI estimation (Jonckheere et al., 2004; Rich
444 et al., 1993). To minimize this error, images were
445 processed according to the methods proposed by Leblanc
446 et al. (2005). All images were analyzed in the same way
447 by one person to ensure the consistency of classification.
448 Each image was divided into 10 rings (each ring has a 9°
449 zenith angle range) and each ring was analyzed
450 separately for determining the two thresholds to
451 minimize the influence of sky luminance heterogeneity,
452 vignetting properties of lenses and multiple scattering in
453 the canopy (Wagner, 2001). The exposure setting affects
454 the division of pixels among the sky, foliage, and mixed
455 classes. It is found that the foliage in the $45\text{--}60^\circ$ zenith
456 angle is least affected by multiple scattering (Leblanc and
457 Chen, 2001). Accordingly, the thresholds for rings within
458 the zenith angle range from 45 to 63° were investigated
459 first to find the range of thresholds and then to provide
460 references for thresholds of other rings.

461 Series of photographs were processed and the DN of
462 two thresholds for each ring were exported to calculate
463 the gap fraction of each ring and the whole image, the
464 mean DN values of sky, foliage and mixed pixels of
465 each ring and the whole image. The contrast between
466 sky and foliage pixels of each ring and whole image
467 were further calculated to analyze the effects of
468 exposure and to explore the optimal exposure.

4. Results and analysis

4.1. The effects of exposure on LAI and gap fraction estimations

Digital hemispherical photographs taken with different exposures are visually different. Fig. 3 demonstrates the photographs with the fixed aperture F5.3 and varying shutter speeds 1/60, 1/125, 1/250, 1/500, 1/1000, and 1/2000 s taken in the Douglas-Fir stand on Vancouver Island. It is visually apparent that with the increase in exposure, the image brightness increases. The decrease in exposure (increasing shutter speed) diminishes the image sharpness. The edges of leaves and tree branches blur due to the light scattering and diffraction. This makes it difficult to distinguish bright leaves from relatively small and underexposed gaps, and can lead to estimation biases for leaf area index and gap fraction.

Photographic exposure influences the magnitude of the canopy gap fraction. Fig. 4 shows variations of gap fraction with exposure for the four forest stands. The sky reference exposure is denoted as 0, and the relative increases of exposure from the sky reference are denoted as 1–7 stops of relative exposure. It can be seen that as the exposure increases, the gap fraction increases almost linearly. Take the series of photographs from the Douglas-Fir stand as an example, when the shutter speed decreases from 1/2000 to 1/60 s, the gap fraction increases from 2.9 to 10.4%.

Conversely, the effective leaf area index L_e decreases with the increase in exposure. Increases of gap fraction with exposure cause increases in estimated global radiation penetration and loss of leaf area. Fig. 5 shows variations of L_e inverted from digital hemispherical photographs with exposure. When the shutter speed decreases from 1/2000 to 1/60 s, L_e of the Douglas-Fir stand decreases correspondingly from 5.16 to 2.40.

The effects of exposure on gap fraction and L_e agree with previous findings from film-based cameras (Chen et al., 1991; Macfarlane et al., 2000). For canopies with large gap fractions, the influences of exposure on the gap fraction and L_e are small (see Figs. 4c and 5c). However, for closed canopies, such as the sugar maple stand in Haliburton Forest (Figs. 4a and 5a) and Douglas-Fir stand on Vancouver Island (Figs. 4b and 5b), the estimated gap fraction and L_e vary dramatically with exposure. For example, at the No. 2 flag in the Douglas-Fir stand, when the relative exposure increases from 1/1000 to 1/500, 1/250, 1/125, and 1/60 s, the gap fraction increases by 19, 48, 108, and 185%, while the L_e decreases by 12, 24, 39, and 50%, respectively. All

469

470

471

472

473

474

475

476

477

478

479

480

481

482

483

484

485

486

487

488

489

490

491

492

493

494

495

496

497

498

499

500

501

502

503

504

505

506

507

508

509

510

511

512

513

514

515

516

517

518

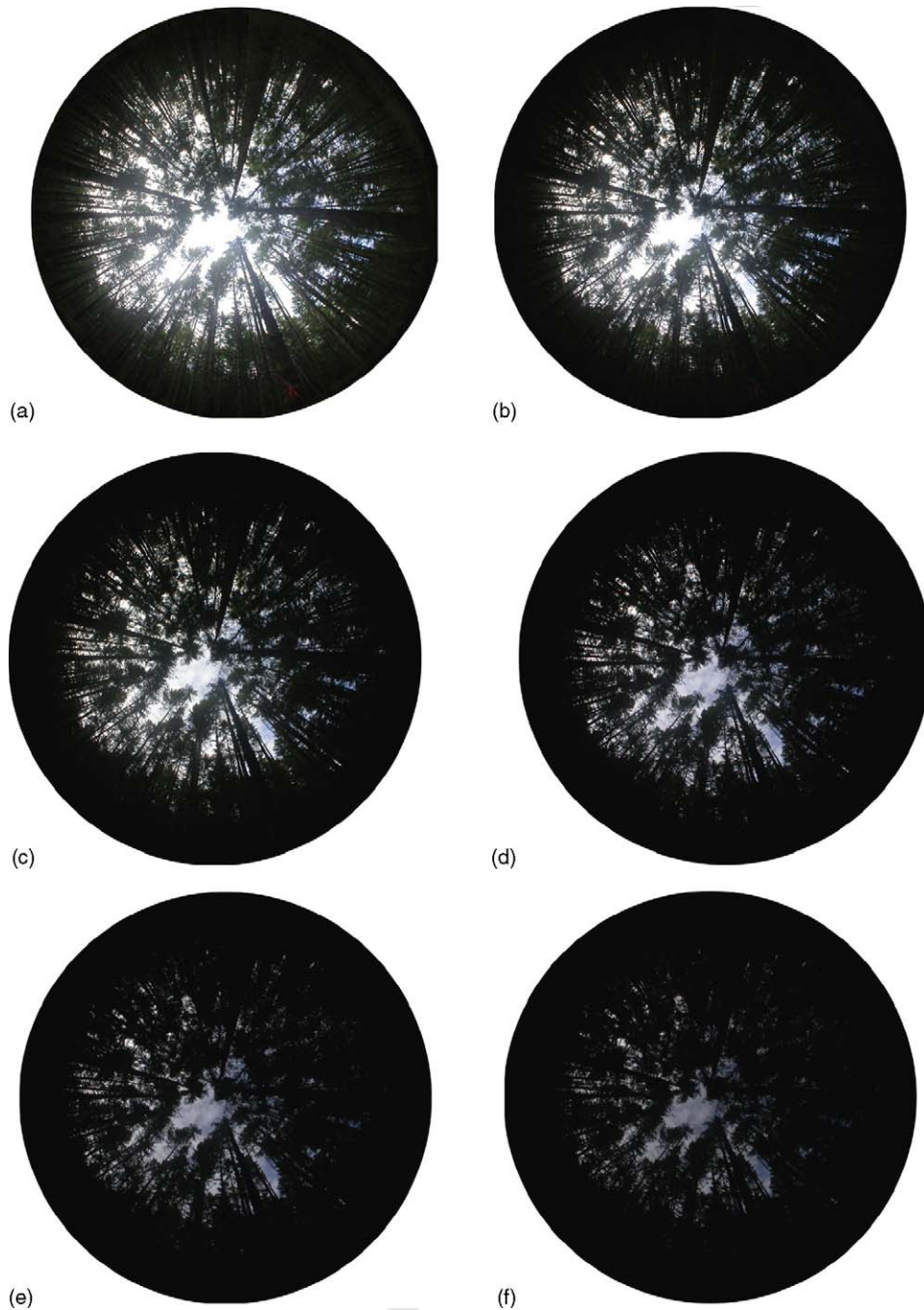


Fig. 3. The influence of photographic exposure. The aperture was fixed at F5.3, and photographs were taken with different shutter speeds. The gap fraction decreases visually from the photograph with the 1/60 s shutter speed to the photograph with the 1/2000 s shutter speed. (a) Hemispherical photograph taken with 1/60 s shutter speed; (b) hemispherical photograph taken with 1/125 s shutter speed; (c) hemispherical photograph taken with 1/250 s shutter speed; (d) hemispherical photograph taken with 1/500 s shutter speed; (e) hemispherical photograph taken with 1/1000 s shutter speed; (f) hemispherical photograph taken with 1/2000 s shutter speed.

518

519 the photos from these four sites showed that increasing
 520 one stop of exposure results in 14–26% differences in L_e
 521 for the Douglas-Fir site, and 7–22% for the sugar maple
 522 site. The difference in L_e varies from 3 to 28% for the

522

523 SB1 site, and 10–20% for the SB2 site. Therefore,
 524 determining an appropriate photographic exposure is
 525 critical to accurately estimate the leaf area index and
 526 gap fraction from hemispherical photographs.

523

524

525

526

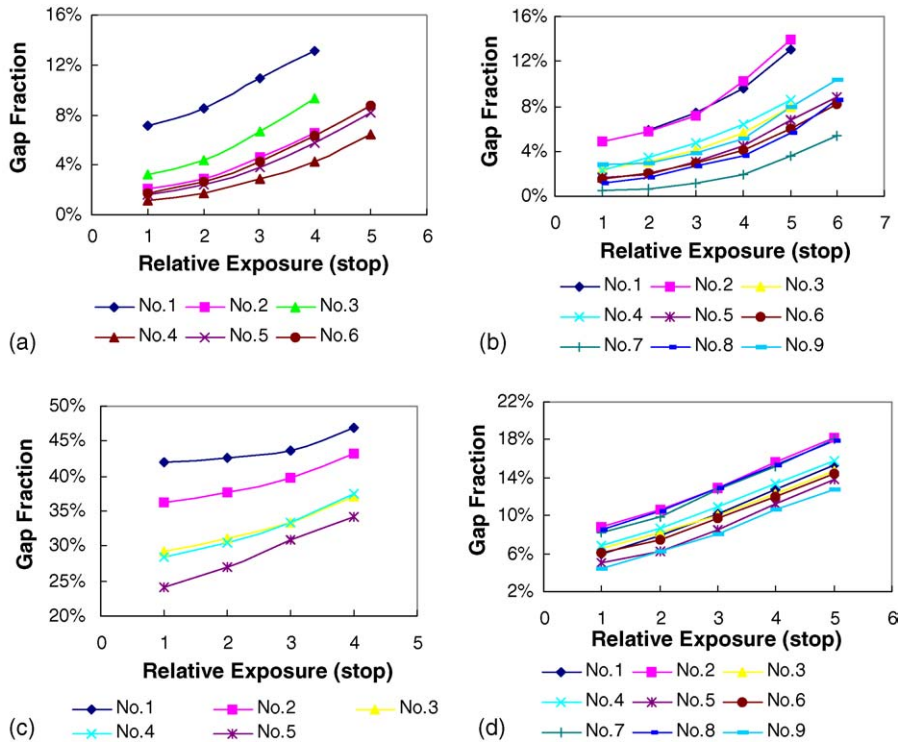


Fig. 4. Variations of gap fraction with the exposure. Hemispherical photographs were taken adjacent to forest flags (denoted as No.) with different exposure schemes at (a) a sugar maple stand in Haliburton Forest; (b) a Douglas-Fir stand on Vancouver Island; (c) a black spruce stand (SB1) in Sudbury; (d) a black spruce stand (SB2) in Sudbury. The relative exposure 0 represents the sky reference, and 1–7 represent 1–7 stops of more exposure relative to the sky reference.

526

4.2. The ideal exposure setting

527

528 One criterion for determining the optimum exposure
 529 would be to maximize the difference between the mean
 530 DN of sky pixels and that of foliage pixels, i.e. the
 531 contrast between these two classes of pixels is the
 532 greatest. The leaf area index and gap fraction calculated
 533 from the automatic exposure and other exposure
 534 schemes were compared to investigate the optimum
 535 exposure for accurate leaf area index estimation. Fig. 6
 536 demonstrates the variations of the mean DN of sky
 537 pixels, foliage pixels, mixed pixels and the DN range
 538 between sky and foliage pixels with exposure. With the
 539 increase in exposure, the mean DN of sky, foliage and
 540 mixed pixels increases. The contrast between foliage
 541 and sky pixels also increases. The error of misclassi-
 542 fication can be reduced with the increase in image
 543 contrast. Although there is an evidence that non-linear
 544 mixing occurs, particularly for component DN values
 545 with high contrasts, the error will clearly increase with a
 546 diminishing dynamic range (Borel and Gerstl, 1994).
 547 The variation of the DN range between foliage and sky
 548 pixels with exposure follows an approximate parabolic

548

549 shape. With a further increase in exposure, the sky
 550 pixels reach the maximum brightness and saturate,
 551 while the brightness of foliage and mixed pixels
 552 continues to increase. The DN difference between these
 553 two categories of pixels reaches the maximum and then
 554 decreases with further increases in exposure.

555 With the gradual change in exposure, the inter-
 556 mediate gray levels, i.e. mixed pixels with the sky and
 557 foliage components, are of particular concern. The
 558 fraction of pixels that are mixed increases greatly
 559 (Fig. 7). The sub-pixel proportions of foliage and sky in
 560 these pixels are determined through a linear unmixing
 561 procedure, given the thresholds representing the ‘pure’
 562 sky and foliage (Leblanc et al., 2005).

563 The DN differences between foliage and sky pixels
 564 of all photographs were calculated to explore the
 565 optimum exposure. Fig. 8a shows the variation of the
 566 DN range with exposure for the sugar maple site in
 567 Haliburton Forest. Considering the sky reference
 568 change (1/500 s at the beginning and 1/250 s at the
 569 end of the measurements), the sky references for the
 570 first series of three photographs were taken as 1/500 s
 571 and the last series of three as 1/250 s. Among several

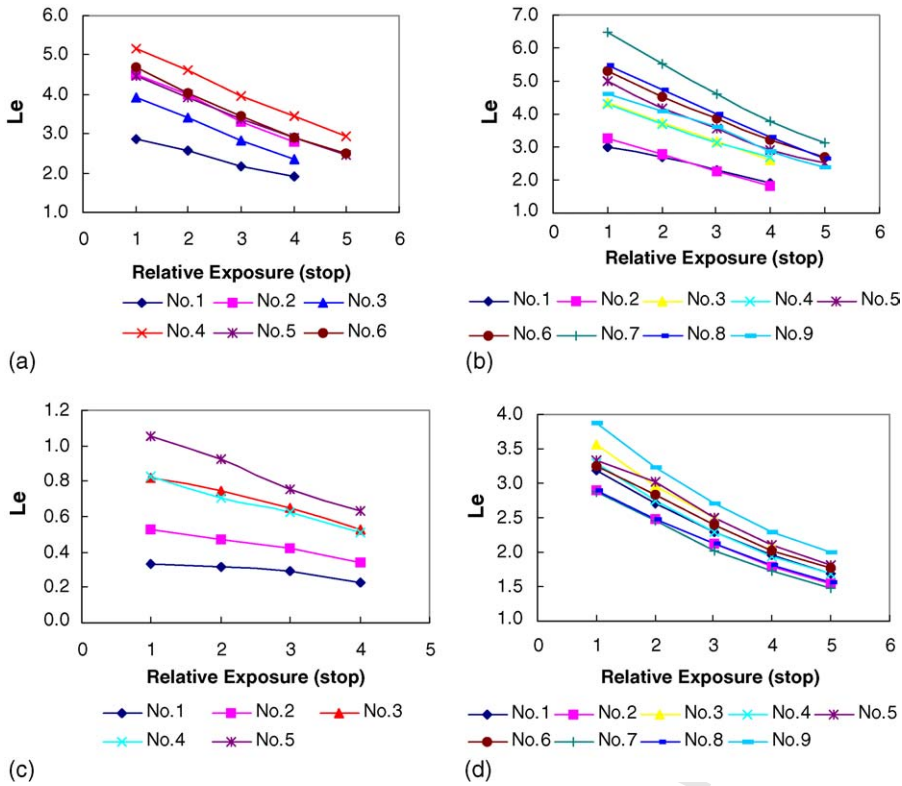


Fig. 5. Variations of effective leaf area index (L_e) with the relative exposure. Hemispherical photographs were taken adjacent to forest flags with different exposure schemes at: (a) a sugar maple stand in Haliburton Forest; (b) a Douglas-Fir stand on Vancouver Island; (c) a black spruce stand (SB1) in Sudbury; (d) a black spruce stand (SB2) in Sudbury. The relative exposure 0 represents the sky reference, and 1–7 represent 1–7 stops of more exposure relative to the sky reference.

571 series of six photographs, the series at locations Nos. 1,
 572 4, 5, and 6 reach the largest image contrast with a two-
 573 stop overexposure relative to the sky reference. Series at
 574 other two locations, Nos. 3 and 4 have the maximum
 575 contrast at three stops of overexposure.
 576

576 Fig. 8b shows the results from the Douglas-Fir stand
 577 on Vancouver Island. All images from nine locations
 578 reach the maximum contrast at 1/250 s, which is three
 579 stops overexposure relative to the sky reference.
 580 Photographs from two locations, Nos. 8 and 9, reach
 581

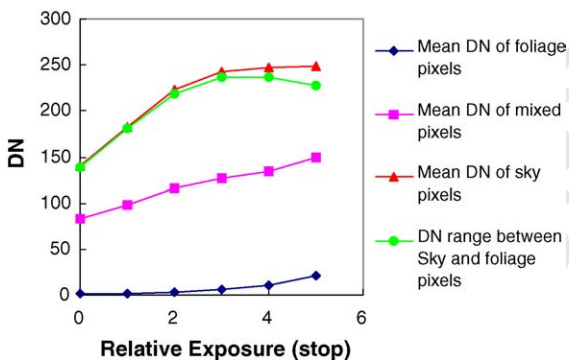


Fig. 6. Variations of mean DN for sky pixels, foliage pixels, mixed pixels, and range between sky and foliage pixels with the relative exposure. The relative exposure 0 represents the sky reference, and 1–5 represent 1–5 stops of more exposure relative to the sky reference.

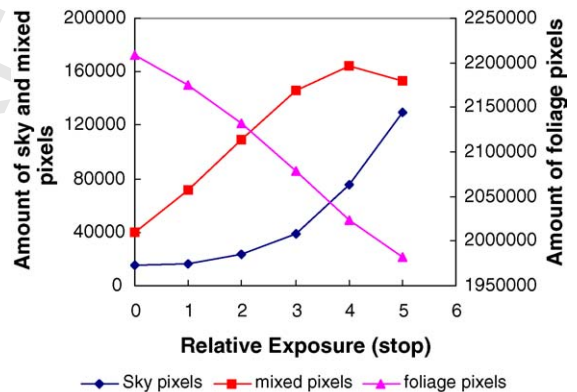


Fig. 7. Variations of the amount of sky pixels, foliage pixels, mixed pixels with relative exposure. The relative exposure 0 represents the sky reference, and 1–5 represent 1–5 stops of more exposure relative to the sky reference.

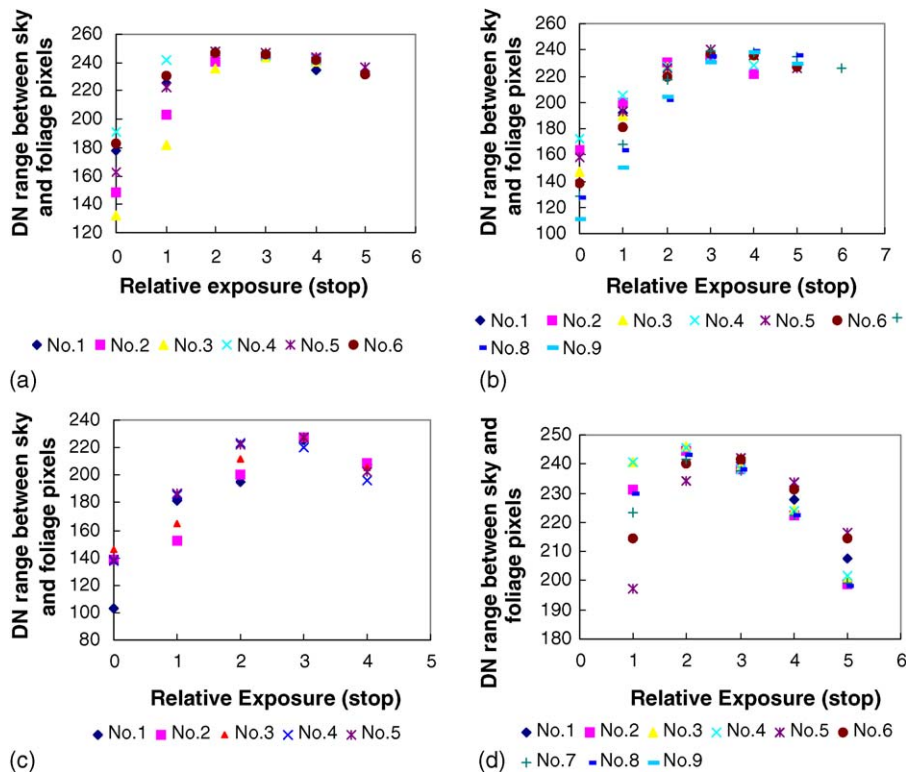


Fig. 8. Variations of the image contrast with the exposure for: (a) a sugar maple stand in Haliburton Forest; (b) a Douglas-Fir stand on Vancouver Island; (c) a black spruce stand (SB1) in Sudbury; (d) a black spruce stand (SB2) in Sudbury. The relative exposure 0 represents the sky reference, and 1–7 represent 1–7 stops of more exposure relative to the sky reference.

581
582 the maximum contrast at 1/125 s. The sky exposure was
583 measured as 1/1000 s right after taking these two series
584 of the photographs. Considering the changes of the sky
585 brightness and the timing of reference measurements,
586 the sky reference for these two series of photographs
587 should be 1/1000 s instead of 1/2000 s taken at the
588 beginning of measurements. So for these two locations,
589 three stops of more exposure result in the largest image
590 contrast as well.

591 For the SB1 stand, three stops of overexposure (1/
592 125 s) relative to sky reference provides the largest
593 image contrast for four locations, Nos. 1, 2, 3, and 5,
594 and two stops of overexposure (1/250 s) for one location
595 No. 4 (See Fig. 8c).

596 Nine series of photographs were taken for the SB2
597 stand. The largest image contrast was found at 1/250 s
598 (two stops of overexposure relative to the sky
599 reference) for eight of nine series of photographs,
600 and three stops of overexposure for one series of
601 photographs (Fig. 8d).

602 It can be concluded that an increase of exposure by
603 2–3 stops from the sky reference exposure produces the
604 largest sky-foliage contrast. The results agree with the

604 finding from film-based hemispherical photographs 605
606 (Chen et al., 1991). Although the exposure inside 607
608 canopies depends on the relative contributions of the 609
610 sky and canopy to the total hemispherical solid angles, 611
612 the extent of relative overexposure inside the canopy is 613
614 independent of canopy openness because the camera 615
616 light meter auto-exposure fixes the open reference sky 617
618 as an 18% mid-grey body. To make the sky appear 619
620 white, two–three stops of overexposure relative to the 621
622 open sky reference exposure can theoretically satisfy 623
624 this requirement. The experiments in sparse and close 625
626 canopies confirm that this exposure scheme can produce 627
628 the largest image contrast for canopies of different 629
630 openness. 631

4.3. The effect of automatic exposure

619 The photographs taken with automatic exposure and
620 the exposure giving the largest image contrast are
621 visually different in terms of image brightness and
622 sharpness. The difference can be easily seen from the
623 photographs taken in the deciduous stand. Fig. 9 shows
624 the photographs taken with the automatic exposure and
625

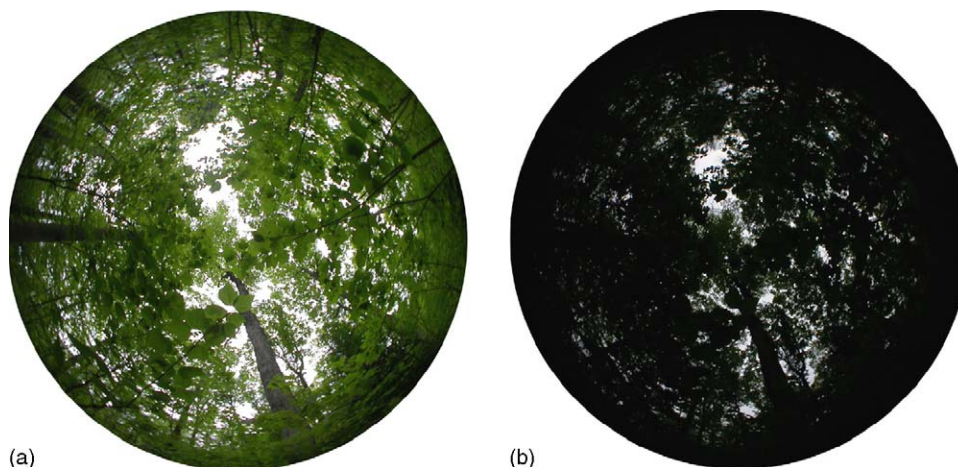


Fig. 9. Comparison for the photograph taken with automatic exposure and the photograph taken with the exposure that produces the largest image contrast (a): digital hemispherical photograph taken with the automatic exposure, showing the composite canopy and sky scene as a 18% grey body (b): digital hemispherical photograph taken with the exposure that producing the largest contrast, making the foliage appear dark but in the mean time allowing the sky to appear white.

625
626 two stops of overexposure with reference to the open
627 sky in the Haliburton Forest stand. Photographs taken
628 with the automatic exposure are much brighter than
629 counterpart taken with the exposure for the largest sky-
630 foliage contrast. Visually, the foliage taken with the
631 automatic exposure appears green, while it appears
632 black in the counterpart with the largest contrast.
633 Canopy gaps in photographs acquired with automatic
634 exposure are visually larger than those in the counter-
635 part, thus resulting in an overestimation of gap fraction
636 and an underestimation of L_e .

637 **Table 1** provides a summary of L_e and gap fraction
638 estimated from photographs with the automatic exposure
639 and with exposure producing the largest sky-foliage
640 contrast for these four sites. For medium to closed
641 canopies, the photographs with automatic exposure
642 underestimate the L_e by 11–71% compared with the
643 photographs with the largest contrast. It shows that for the
644 SB2 stand, the automatic exposure is one stop larger than
645 the exposure producing the largest image contrast. For
646 the sugar maple stand in Haliburton Forest and the
647 Douglas-Fir stand, the automatic exposure is larger than
648 the largest contrast exposure by 1–2 stops. The difference
649 can be as large as three stops for portions of canopies that
650 have large L_e values and thus small gap fractions. For
651 example, the automatic exposure at the No. 7 of the
652 Douglas-Fir site is three stops larger than the exposure
653 that produces the largest contrast. The mean L_e values
654 derived from photographs with the automatic exposure
655 and largest contrast are 2.69 and 4.61, and the gap
656 fractions are 1.98 and 7.29%, respectively. For this
657 location, the L_e is underestimated by 71% if the automatic
658 exposure setting is used.

658
659 The results from the sugar maple, Douglas-Fir, and
660 SB2 stands demonstrate that digital hemispherical
661 photographs taken with automatic exposure can result
662 in underestimations of L_e in medium to dense
663 canopies. But the estimations from open canopies
664 had an opposite trend. In sparse canopies, the
665 contribution of sky pixels is much larger than that
666 of foliage pixels. So under the same sky brightness
667 conditions, the whole scene of sparse canopies is
668 much brighter than that of closed canopies. The
669 camera automatically images sparse canopies with
670 less exposure, i.e. the automatic exposure would be
671 less than two stops of overexposure relative to the sky
672 reference. Thus the foliage is under-exposed com-
673 pared with closed canopies, which leads to losses of
674 many small canopy gaps and consequently an
675 overestimation of L_e . For the SB1 stand, the automatic
676 exposure underexposes the photographs by 1–2 stops,
677 resulting in L_e overestimations by 14–42% and gap
678 fraction underestimations by 4–22%. Therefore, the
679 automatic exposure can be particularly problematic in
680 either very open or very closed canopies.

4.4. Comparison of L_e from different instruments

681
682 To test whether two or three stops of overexposure
683 relative to the sky reference is the optimum exposure for
684 leaf area index estimation, L_e derived from digital
685 hemispherical photographs described previously was
686 evaluated in comparison with the corresponding L_e
687 values measured at same locations by the LAI-2000
688 instrument. The LAI-2000 measures the blue light
689 (400–490 nm) attenuation through the canopy at five

Table 1
Comparisons between the automatic exposure and the exposure producing the largest sky-foliage contrast

Stand	Location (No.)	Exposure		L_e Result from		Gap fraction	
		Automatic	Largest contrast	Automatic exposure	Exposure with largest contrast	Automatic exposure (%)	Exposure with largest contrast (%)
Sugar Maple stand in Haliburton Forest	1	1/60	1/125	2.181	2.552	10.92	8.54
	2	1/30	1/60	2.801	3.298	6.58	4.59
	3	1/30	1/60	2.347	2.807	9.35	6.72
	4	1/15	1/60	2.925	3.964	6.50	2.88
	5	1/8	1/60	2.671	4.263	8.17	2.37
	6	1/8	1/60	2.493	4.031	8.80	2.70
Douglas-Fir stand in Vancouver	1	1/125	1/250	1.907	2.288	13.09	9.66
	2	1/125	1/250	1.828	2.267	13.93	10.19
	3	1/125	1/250	2.624	3.154	7.97	5.67
	4	1/125	1/250	2.691	3.130	8.52	6.37
	5	1/60	1/250	2.507	3.563	8.87	4.49
	6	1/60	1/250	2.711	3.876	8.21	4.13
	7	1/30	1/250	2.698	4.613	7.29	1.98
	8	1/60	1/125	2.635	3.285	8.54	5.58
	9	1/60	1/125	2.400	2.860	10.39	7.99
Black Spruce (SB1) stand in Sudbury	1	1/500	1/125	0.329	0.293	41.96	43.68
	2	1/500	1/125	0.524	0.419	36.25	39.80
	3	1/500	1/125	0.820	0.650	29.15	33.32
	4	1/1000	1/250	0.911	0.705	26.54	30.49
	5	1/500	1/125	1.055	0.752	24.10	30.99
Black Spruce (SB2) stand in Sudbury	1	1/125	1/250	2.295	2.714	10.16	7.87
	2	1/125	1/250	2.118	2.470	12.97	10.68
	3	1/125	1/250	2.497	2.948	10.06	8.25
	4	1/125	1/250	2.285	2.740	10.99	8.72
	5	1/125	1/250	2.503	2.825	8.54	6.21
	6	1/125	1/250	2.387	2.835	9.74	7.43
	7	1/125	1/250	2.031	2.460	12.71	9.87
	8	1/125	1/250	2.127	2.486	12.84	10.45
	9	1/125	1/250	2.711	3.224	8.05	6.27

689

concentric rings: 0–13°, 16–28°, 32–43°, 47–58°, and 61–74° (Li-Cor, 1992). The ratio of the below to above canopy readings for each ring is measured to obtain the gap fraction of each ring and the effective leaf area index.

694

695

696

697

698

699

700

701

702

According to the LAI-2000 instrument, L_e was 4.84 for the sugar maple stand on May 27, 2004, and 3.93, 1.26, and 3.20 for the Douglas-Fir, SB1 and SB2 stands, respectively. For the purpose of comparison, hemispherical photographs at the zenith angles from 0 to 75° of were used to calculate L_e , which matches the angle range of the LAI-2000. The root mean square error (RMSE) is calculated to estimate the deviation between two measurements:

703

$$\text{RMSE} = \sqrt{\frac{1}{n} \sum_{i=1}^n (\hat{y}_i - y_i)^2} \quad (2)$$

where \hat{y}_i and y_i are the L_e values estimated from the LAI-2000 and hemispherical photographs, respectively, and n is the number of locations where the measurements were taken.

Fig. 10a demonstrates that the L_e values estimated from photographs with automatic exposure correlates with those from the LAI-2000 ($R^2 = 0.77$). But compared with the LAI-2000, the hemispherical photographs with automatic exposure underestimate L_e , especially for closed canopies. L_e estimated from hemispherical photographs deviates that from the LAI-2000. The RMSE between two measurements is 1.26. Comparisons for other canopies also confirmed that digital hemispherical photographs underestimate L_e (van Gardingen et al., 1999). Fig. 10b shows the comparison of L_e values from LAI-2000 and hemispherical photographs with the largest contrast. With the increase in image contrast, the correlation and the

703

704

705

706

707

708

709

710

711

712

713

714

715

716

717

718

719

720

721

722

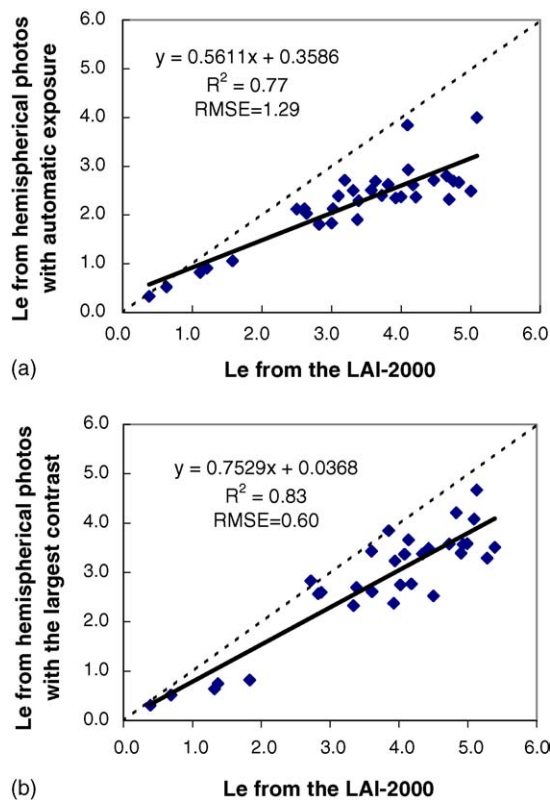


Fig. 10. Relationship between L_e derived from the LAI-2000 and from digital hemispherical photographs (the dotted line is 1:1 line): (a) L_e from the LAI-2000 and digital hemispherical photographs with the automatic exposure; (b) L_e from the LAI-2000 and digital hemispherical photographs with the largest contrast.

722

723 accuracy of L_e estimations from hemispherical
724 photographs are both improved ($R^2 = 0.83$, RMSE
725 = 0.60). Compared with LAI-2000 measurements,
726 photographs with automatic exposure underestimate
727 L_e by 48.7% on average, while photographs with
728 largest image contrasts underestimate L_e by 23.1% on
729 average.

730 We analyze all 10 rings of hemispherical photo-
731 graphs to investigate whether two or three steps of
732 overexposure can create the largest image contrast for
733 all zenith angles. Contrasts between sky and foliage
734 pixels for every 9° annulus rings were calculated and
735 compared separately. In near-vertical directions,
736 canopies generally have large gap fractions and thus
737 the light intensity is high. It is found that at three steps
738 of overexposure, ring 1 or 2 tends to be saturated though
739 the whole image reaches the largest contrast. Generally,
740 when the whole image reaches the maximum contrast,
741 sections at small zenith angles are overexposed by one
742 step, resulting in underestimations of the foliage area in
743 near-vertical directions. The overexposure in the near-

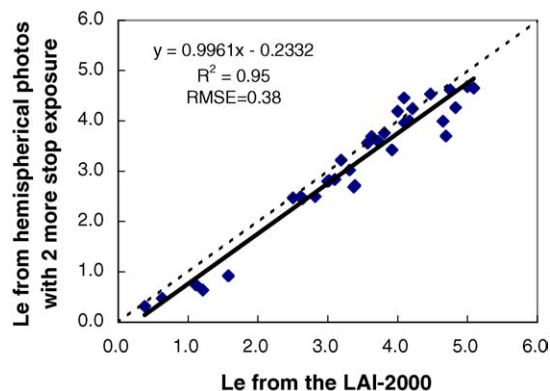


Fig. 11. Relationship between L_e values derived from the LAI-2000 and digital hemispherical photographs with two stops of more exposure relative to the sky automatic exposure (the dotted line is 1:1 line).

743

744 vertical direction may be due to the multiple scattering
745 inside the canopy. Chen et al. (1991) demonstrated that
746 film-based photographs are overexposed at small
747 zenith angles and underexposed at large zenith angles
748 where gaps are small and the probability of viewing top
749 foliage is low. As in our analysis, only zenith angles
750 below 75° were included for comparisons, the under-
751 exposure in near horizontal directions has been
752 eliminated. Therefore, to avoid overexposure in near-
753 vertical directions, all the photographs at the two stops
754 of overexposure were compared with those from the
755 LAI-2000. Compared with the photographs with the
756 largest contrast, the photographs with two stops of
757 overexposure compensate the overexposure in near-
758 vertical directions and thus produce larger L_e values
759 (Fig. 11). The correlation and accuracy of L_e
760 estimations are greatly improved ($R^2 = 0.95$, and
761 RMSE = 0.38). It is found that at two stops of
762 overexposure, the image contrast is actually very close
763 to the maximum contrast. Therefore, two stops of
764 overexposure relative to the sky reference is the
765 optimum exposure of digital photographs for accurate
766 estimation of LAI. A zenith angle range from 0 to 75° is
767 recommended to avoid the underexposure in near
768 horizontal directions.

769 5. Discussion and suggested measurement 770 protocol

771 Overexposure by two stops relative to the sky
772 reference is determined to be the optimum exposure
773 for digital photographs for LAI measurements based
774 on the comparison with the LAI-2000 measurements.
775 Though the LAI-2000 tends to underestimate LAI
776 (Battaglia et al., 1998; Chen, 1996a; Kalácska et al.,
777 2005), this is mostly due to foliage clumping (Chen,

777
778 1996b). Multiple scattering of blue light within the
779 canopy could have similar effects on the gap fraction
780 determination using both LAI-2000 and fish-eye
781 photography, but would not influence considerably
782 their intercomparison. The reason for using two stops
783 rather than theoretical 2.5–3 stops (Chen et al., 1991;
784 Wagner, 2001) is clearly the need to minimize the
785 effect of strong scattering of light by foliage near the
786 vertical direction. From the above analysis, it should
787 be noted that finding the optimum exposure to obtain
788 the correct leaf area index is actually a balancing act
789 between the overexposure near-vertical directions and
790 underexposure near horizontal directions. This may be
791 an inherent limitation of hemispherical photography
792 technique for canopy structural measurements.
793 Because of the non-uniform effect of exposure across
794 the zenith angle range, the inversion of leaf angle
795 distribution using gap fractions at various zenith
796 angles can still be distorted even when the optimum
797 exposure is found (Chen et al., 1991). Until this
798 exposure angular effect is resolved, the hemispherical
799 photographic technique should only remain as a proxy
800 measurement technique. Furthermore, variations of
801 the sky conditions during measurements need to be
802 taken into consideration. Stable sky conditions are
803 ideal for taking hemispherical photographs. Near
804 sunrise or sunset, the sky brightness could vary and the
805 correct exposure inside the canopy needs to be
806 changed accordingly. When the plot is large or the
807 sky condition is not stable, recording the sky reference
808 before and after the measurements is necessary for
809 determining the correct exposure. Two photographs
810 are recommended for each location, with two stops
811 and one stop or three stops of more exposure
812 depending on the change of sky brightness. Determining
813 the optimum exposure based on the sky brightness,
814 although it is physically meaningful, can sometimes
815 be difficult to implement in the field because it is often
816 not possible to find a very large open field in a forested
817 area. With some experience, the sky brightness can be
818 measured from inside the stand using a tele-lens
819 through a large canopy gap. Using spot meter with a
820 narrow angle of view is practical to measure the sky
821 luminance in this case (Clearwater et al., 1999;
822 Wagner, 2001). Although sky brightness can some-
823 times be variable in different directions, it will take a
824 50% difference in sky brightness to change the
825 exposure by one stop. Therefore, taking the measure-
826 ments in one or two gaps is normally sufficient,
827 although all reference measurements are made in large
828 opening areas for the purposes of this study. Based on
829 results of this research, we propose the following

829
830 protocol in using digital cameras for plant canopy
831 structural measurements:

- 832
833 1. to determine the sky exposure. The ideal determina-
834 tion would be using the same camera with the same
835 fish-eye lens in a very large opening with no
836 obstructions above 15° of the elevation angle in all
837 directions. In case this is not possible, similar
838 measurements can be made in large canopy gaps
839 using a tele-lens, but in this case precautions should
840 be taken for directional variability of sky brightness.
841 The preferred aperture is F5.3 or similar. 842
- 843 2. to determine the in-stand exposure by increasing the
844 shutter speed by two stops with the aperture unchanged
845 at F5.3. For example, if the sky reference is F5.3 and
846 S1000 (i.e. speed of 1/1000 s), the correct exposure
847 inside the stand is F5.3 and S250. This exposure setting
848 is not influenced by the density of the stand. 849
- 850 3. to distinguish sky and foliage in the digital
851 photograph by finding two thresholds, one for pure
852 sky and one for pure foliage, with brightness in
853 between as mixed sky and foliage. A software which
854 is capable of unmixing the mixed pixels should be
855 used (Leblanc et al., 2005). 856

857 6. Conclusion

858
859 Correct exposure is the key to taking digital
860 hemispherical photographs for accurate estimation of
861 L_e , clumping index and the actual LAI. Photographic
862 exposure affects LAI and gap fraction retrievals even if no
863 saturation occurs. Automatic exposure for collection of
864 digital photographs is unreliable for the LAI estimation.
865 Photographs taken with the automatic exposure under-
866 estimate L_e in medium to dense canopies and overestimate
867 L_e in very open canopies. This paper proposed a protocol
868 for acquiring digital hemispherical photographs under
869 various sky brightness conditions and in canopies with
870 different closures. Two stops of overexposure relative to
871 the sky reference is proven theoretically and experimen-
872 tally to be the optimum exposure for taking digital
873 hemispherical photographs for the purposes of obtaining
874 the mean canopy gap fraction and the effective LAI.
875 Taking LAI-2000 measurements as a standard for
876 comparison, the proposed optimum exposure greatly
877 improves the accuracy of L_e estimates relative to those
878 with automatic exposure.

879 Acknowledgements

880 The research was financed by the GEOIDE project.
881 We acknowledge the support from Thomas Noland of

881
882 the Ontario Forest Research Institute for the field
883 measurements. Assistance of Gang Mo, Mingzhen
884 Chen, and Oliver Sonnentag in the field is greatly
885 appreciated. Dr. Carl Menges made useful comments on
886 an early version of the manuscript.

References

- 887
888 Amiro, B.D., Chen, J.M., Liu, J., 2000. Net primary productivity
889 following forest fire for Canadian ecoregions. *Can. J. Forest Res.*
890 30, 939–947.
- 891 Battaglia, M., Cherry, M.L., Beadle, C.L., Sands, P.J., Hingston, A.,
892 1998. Prediction of leaf area index in eucalypt plantations: effects
893 of water stress and temperature. *Tree Physiol.* 18, 521–528.
- 894 Blennow, K., 1995. Sky view factors from high-resolution scanned
895 fish-eye lens photographic negatives. *J. Atmos. Ocean. Technol.*
896 12, 1357–1362.
- 897 Borel, C.C., Gerstl, S.A.W., 1994. Nonlinear spectral mixing models
898 for vegetative and soil surfaces. *Remote Sens. Environ.* 47, 403–
899 416.
- 900 Brenner, A.J., Cueto Romero, M., Garcia Haro, J., Gilabert, M.A.,
901 Incoll, L.D., Martinez Fernandez, J., Porter, E., Pugnaire, F.I.,
902 Younis, M.T., 1995. A comparison of direct and indirect methods
903 for measuring leaf and surface-area of individual bushes. *Plant*
904 *Cell Environ.* 18, 1332–1340.
- 905 Bunsen, R., Roscoe, H., 1862. Photochemische Untersuchungen. *Ann.*
906 *Phys. Chem.* 117, 529–562.
- 907 Chen, J.M., 1996a. Canopy architecture and remote sensing of the
908 fraction of photosynthetically active radiation in boreal conifer
909 stands. *IEEE Trans. Geosci. Remote Sens.* 34, 1353–1368.
- 910 Chen, J.M., 1996b. Optically-based methods for measuring seasonal
911 variation in leaf area index of boreal conifer forests. *Agric. Forest*
912 *Meteorol.* 80, 135–163.
- 913 Chen, J.M., Black, T.A., Adams, R.S., 1991. Evaluation of hemi-
914 spherical photography for determining plant area index and geo-
915 metry of a forest stand. *Agric. Forest Meteorol.* 56, 129–143.
- 916 Chen, J.M., Black, T.A., 1992. Defining leaf area index for non-leaf
917 leaves. *Plant Cell Environ.* 15, 421–429.
- 918 Chen, J.M., Liu, J., Cihlar, J., Guolden, M.L., 1999. Daily canopy
919 photosynthesis model through temporal and spatial scaling for
920 remote sensing applications. *Ecol. Model.* 124, 99–119.
- 921 Chen, J.M., Rich, P.M., Gower, S.T., Norman, J.M., Plummer, S.,
922 1997. Leaf area index of boreal forests: theory, techniques,
923 and measurements. *J. Geophys. Res. Atmos.* 102 (D24),
924 29429–29443.
- 925 Clearwater, M.J., Nifinluri, T., van Gardingen, P.R., 1999. Forest fire
926 smoke and a test of hemispherical photography for predicting
927 understorey light in Bornean tropical rain forest. *Agric. Forest*
928 *Meteorol.* 97, 129–139.
- 929 Covington Innovations, 2004, [http://www.covingtoninnovations.com/
930 dslr/Curves.html](http://www.covingtoninnovations.com/dslr/Curves.html).
- 931 Digital Photography Review, 2003, <http://www.dpreview.com/>.
- 932 Easter, M.J., Spies, T.A., 1994. Using hemispherical photography for
933 estimating photosynthetic photon flux density under canopies and
934 in gaps in Douglas-Fir forests of the Pacific northwest. *Can. J.*
935 *Forest Res.* 24, 2050–2058.
- 936 Englund, S.R., O'Brien, J.J., Clark, D.B., 2000. Evaluation of digital
937 and film hemispherical photography and spherical densitometry
938 for measuring forest light environments. *Can. J. Forest Res.* 30
939 (12), 1999–2005.
- Fassnacht, K.S., Gower, S.T., Norman, J.M., McMurtric, E.R., 1994. A
940 comparison of optical and direct methods for estimating foliage
941 surface area index in forests. *Agric. Forest Meteorol.* 71, 183–207.
942
- Fournier, R.A., Landry, R., August, N.M., Fedosejevs, G., Gauthier,
943 R.P., 1996. Modelling light obstruction in three conifer forests
944 using hemispherical photography and fine tree architecture. *Agric.*
945 *Forest Meteorol.* 82, 47–72.
- Frazer, G.W., Fournier, R.A., Trofymow, J.A., Hall, R.J., 2001. A
947 comparison of digital and film fisheye photography for analysis of
948 forest canopy structure and gap light transmission. *Agric. Forest*
949 *Meteorol.* 109, 249–263.
- Gower, S.T., Kucharik, J.K., Norman, J.M., 1999. Direct and indirect
951 estimation of leaf area index, fapar, and net primary production of
952 terrestrial ecosystems. *Remote Sens. Environ.* 70, 29–51.
953
- Hale, S.E., Edwards, C., 2002. Comparison of film and digital hemi-
954 spherical photography across a wide range of canopy densities.
955 *Agric. Forest Meteorol.* 112, 51–56.
- Jonckheere, I., Fleck, S., Nackaerts, K., Muys, B., Coppin, P., Weiss,
957 M., Baret, F., 2004. Review of methods for in situ leaf area index
958 determination. Part I. Theories, sensors and hemispherical photo-
959 graphy. *Agric. Forest Meteorol.* 121, 19–35.
- Kalácska, M., Calvo-Alvarado, J.C., Sánchez-Azofeifa, G.A., 2005.
961 Calibration and assessment of seasonal changes in leaf area index
962 of a tropical dry forest in different stages of succession. *Tree*
963 *Physiol.* 25, 733–744.
- Kimball, J.S., Thornton, P.E., White, M.A., Running, S.W., 1997.
965 Simulating forest productivity and surface-atmosphere carbon
966 exchange in the BOREAS study region. *Tree Physiol.* 17, 589–
967 599.
- Leblanc, S.G., 2003. Digital Hemispherical Photography Manual,
969 version 1.0 Canada Centre for Remote Sensing, Natural Resources
970 Canada, Ottawa.
- Leblanc, S.G., Chen, J.M., 2001. A practical scheme for correcting
972 multiple scattering effects on optical LAI measurements. *Agric.*
973 *Forest Meteorol.* 110 (2), 125–139.
- Leblanc, S.G., Chen, J.M., Fernandes, R., Deering, D.W., Conley, A.,
975 2005. Methodology comparison for canopy structure parameters
976 extraction from digital hemispherical photography in boreal for-
977 ests. *Agric. Forest Meteorol.* 129, 187–207.
- Li-Cor, I., 1992. LAI-2000 plant canopy analyzer instruction manual.
979 LI-COR Inc., Lincoln, Nebraska, USA.
- Liu, J., Chen, J.M., Cihlar, J., Park, W., 1997. A process-based boreal
981 ecosystems productivity simulator using remote sensing inputs.
982 *Remote Sens. Environ.* 62, 158–175.
- Liu, J., Chen, J.M., Cihlar, J., Chen, W., 2002. Net primary produc-
984 tivity mapped for Canadian at 1-km resolution. *Global Ecol.*
985 *Biogeogr.* 11, 115–129.
- Macfarlane, C., Coote, M., White, D.A., Adams, M.A., 2000. Photo-
987 graphic exposure affects indirect estimation of leaf area in planta-
988 tions of *Eucalyptus globulus* Labill. *Agric. Forest Meteorol.* 100,
989 155–168.
- Machado, J.-L., Reich, P.B., 1999. Evaluation of several measures of
991 canopy openness as predictors of photosynthetic photon flux
992 density in deeply shaded conifer-dominated forest understorey.
993 *Can. J. Forest Res.* 29, 1438–1444.
- Mussche, S., Samson, R., Nachtergale, L., De Schrijver, A., Lemeur,
995 R., Lust, N., 2001. Comparison of optical and direct methods for
996 monitoring the seasonal dynamics of leaf area index in deciduous
997 forests. *Silva Fenn.* 35 (4), 373–384.
- Nilson, T., 1999. Inversion of gap frequency data in forest stands.
999 *Agric. Forest Meteorol.* 98–99, 437–448.

- 1000 Nobis, M., Hunziker, U., 2005. Automatic thresholding for hemi- 1022
 1002 spherical canopy-photographs based on edge detection. *Agric.* 1023
 1003 *Forest Meteorol.* 128, 243–250. 1024
 1004 Norman, K., 2003. Photography Page, [http://www.normankoren.com/](http://www.normankoren.com/digital_tonality.html) 1025
 1005 [digital_tonality.html](http://www.normankoren.com/digital_tonality.html) - Exposure. 1026
 1006 Olsson, L., Carlsson, K., Grip, H., Perttu, K., 1982. Evaluation of 1027
 1007 forest-canopy photographs with diode-array scanner OSIRIS. *Can.* 1028
 1008 *J. Forest Res.* 12, 822–828. 1029
 1009 Rich, P.M., Clark, D.B., Clark, D.A., Oberbauer, S.F., 1993. Long- 1030
 1010 term study of solar radiation regimes in a tropical wet forest using 1031
 1011 quantum sensors and hemispherical photography. *Agric. Forest* 1032
 1012 *Meteorol.* 65, 107–127. 1033
 1013 Ross, J., 1981. *The Radiation Regime and Architecture of Plant* 1034
 1014 *Stands.* Junk, London, pp. 391. 1035
 1015 Roxburgh, J.R., Kelly, D., 1995. Uses and limitations of hemispherical 1036
 1016 photography for estimating forest light environments. *NZ J. Ecol.* 1037
 1017 19 (2), 213–217. 1038
 1018 Running, S.W., Hunt, E.R., 1993. Generalization of a forest eco- 1039
 1019 system process model for other biomes, BIOME-BGC, and 1040
 1020 an application for global scale models scaling physiological 1041
 1021 processes: leaf to globe. Academic Press, San Diego, pp. 1042
 1022 141–158. 1043
 Sommer, K.J., Lang, A.R.G., 1994. Comparative analysis of 2 1023
 indirect methods of measuring leaf area index as applied to 1024
 minimal and spur pruned grape vines. *Aust. J. Plant Physiol.* 21, 1025
 197–206. 1026
 Unwin, D.M., 1980. *Microclimate Measurements for Ecologists.* 1027
 Academic Press, New York. 1028
 van Gardingen, P.R., Jackson, G.E., Hernandez-Daumas, S., Russell, 1029
 G., Sharp, L., 1999. Leaf area index estimates obtained for 1030
 clumped canopies using hemispherical photography. *Agric. Forest* 1031
Meteorol. 94, 243–257. 1032
 Wagner, S., 1998. Calibration of grey values of hemispherical 1033
 photographs for image analysis. *Agric. Forest Meteorol.* 90, 1034
 103–117. 1035
 Wagner, S., 2001. Relative radiance measurements and zenith angle 1036
 dependent segmentation in hemispherical photography. *Agric.* 1037
Forest Meteorol. 107, 103–115. 1038
 Welles, J.M., Norman, J.M., 1991. Instrument for indirect measure- 1039
 ment of canopy architecture. *Agron. J.* 83, 818–825. 1040
 Weiss, M., Baret, F., Smith, G.J., Jonckheere, I., Coppin, P., 2004. 1041
 Review of methods for in situ leaf area index (LAI) determination. 1042
 Part II. Estimation of LAI, errors and sampling. *Agric. Forest* 1043
Meteorol. 121, 37–53. 1044

UNCORRECTED PROOF